IEEE Access
Multidisciplinary : Rapid Review : Open Access Journal

Received May 24, 2018, accepted June 20, 2018, date of publication June 25, 2018, date of current version July 25, 2018.

Digital Object Identifier 10.1109/ACCESS.2018.2850307

Joint Two-Dimensional DOA and Frequency Estimation for L-Shaped Array via Compressed Sensing PARAFAC Method

LE XU[1], RIHENG WU[2], (Member, IEEE), XIAOFEI ZHANG[3,4], AND ZHAN SHI[1]

[1]College of Electronic and Information Engineering, Nanjing University of Aeronautics and Astronautics, Nanjing 210000, China
[2]Department of Information Engineering, Wenjing College, Yantai University, Yantai 264005, China
[3]College of Electronic and Information Engineering, Nanjing University of Aeronautics and Astronautics, Nanjing 210000, China
[4]State Key Laboratory of Millimeter Waves, Southeast University, Nanjing 210096, China

Corresponding author: Riheng Wu (riheng_w@163.com)

This work was supported in part by China NSF under Grant 61371169, in part by Shandong Province NSF under Grant ZR2016FM43, and in part by the Graduate Innovative Base (Laboratory) Open Funding of the Nanjing University of Aeronautics and Astronautics under Grant kfjj20170412.

ABSTRACT In this paper, we combine the compressed sensing theory with the parallel factor (PARAFAC) model to present a 2-D direction of arrival (2D-DOA) and a frequency estimation algorithm for an L-shaped array. We first build the multi-delay outputs data as the PARAFAC model, then compress it with partitioning and perform the PARAFAC decomposition through a trilinear alternating least square algorithm. Finally, we reconstruct the received data with sparsity to obtain the automatically paired 2D-DOA and frequency. The proposed algorithm is effective for both uniform and non-uniform L-shaped array, and owing to the compression process, it holds the properties of lower computational complexity and smaller capacity for data storage, compared with a traditional PARAFAC algorithm. The angle and frequency estimation performance of the proposed algorithm is close to the traditional PARAFAC method, and outperforms the estimating signal parameters via a rotational invariance techniques algorithm and a propagator method. Simulation results verify the effectiveness and superiority of our approach.

INDEX TERMS Direction of arrival (DOA), compressed sensing, frequency, parallel factor (PARAFAC), L-shaped array.

I. INTRODUCTION

Joint multi-parameter estimations of received signals has aroused considerable concerns recently and has been investigated for numerous engineering applications containing radar, sonar, satellite communication and so on [1]–[4]. The direction of arrival (DOA) and frequency estimation is a fundamental problem of array signal processing and is becoming a hot topic. Till now, many novel algorithms have been proposed for the problem of joint DOA and frequency estimation [5]–[13], which includes multiple signal classification (MUSIC) algorithm [5], [6], estimating signal parameters via rotational invariance techniques (ESPRIT) [7], [8], Propagator method (PM) [9]. Compared to MUSIC algorithm which requires multi-dimensional spectrum-peak search, ESPRIT algorithm and PM algorithm provide a reduced computational burden as they have no need for spectrum-peak search. The algorithms mentioned above are all for one-dimensional DOA and frequency estimation, and some other algorithms like unitary ESPRIT in [10], 3D-ESPRIT in [11] and quadrilinear decomposition method mentioned in [12] and [13] can provide two-dimensional direction of arrival(2D-DOA) and frequency estimation.

The trilinear decomposition, which is also referred to as parallel factor (PARAFAC) analysis [14], [15], has been success- fully used to deal with the problem of DOA and frequency estimation. The algorithms proposed in [16] and [17] obtain the DOA and frequency estimation through PARAFAC decomposition of oversampled output, while the PARAFAC method in [18] utilizes the multi-delay outputs to get the angle and frequency estimation. However, the traditional PARAFAC decomposition-based algorithm suffers from heavy computa- tional load as well as large capacity for data storage.

Compressed sensing (CS) [19], [20] has attracted plenty of attention recently, and it has been successfully introduced to image processing, radar imaging, channel estimation and some other fields [21]. According to the compressed sensing theory, a signal can be reconstructed via fewer samples than required by the Nyquist sampling theorem if it's sparse in some domains. Coincidentally, the DOA and frequency of sources form a sparse vector in the potential signal space, therefore, compress- ed sensing is applicable to the problem of joint DOA and frequency estimation [22]. Reference [23] has already proposed an angle and frequency estimation method with linear array via compressed sensing parallel factor(CS-PARAFAC) model, whereas it only can obtain the one-dimensional DOA of received signals.

In this paper, we combine the compressed sensing theory with PARAFAC model and derive an efficient 2D-DOA and frequency estimation algorithm for L-shaped array. The proposed algorithm first constructs the received data for L-shaped array with multi-delay outputs, then to avoid constructing two-dimensional overcomplete dictionary for signal recovery, we make some changes of the compression process in [23] and compress the received data with partition, then utilizes trilinear alternating least square (TALS) algorithm [14], [15] to estimate the compressed parameter matrices. Finally, we obtain the 2D-DOA and frequency estimation via sparsity. For the multi-delay outputs system, we build a delay matrix which changes with the antenna size, and it's implemented via hardware and located behind the RF receiving channel. In addition, we can use the direct RF sampling method of software radio to obtain the digital signal of real carrier frequency.

In our paper, we also evaluate the theoretical performance of angle and frequency estimations for L-shaped array via Cramér-Rao bound (CRB) [24], [26], which is employed as a benchmark for the lower bound on the mean square error (MSE) of unbiased angle and frequency estimation. The main contributions of our research are summarized as follows:

1) We construct the received data for L-shaped array which is suitable for 2D-DOA and frequency estimation.

2) we improve the compression process in [23] and compress the PARAFAC model of received data with partition, which avoids two-dimensional overcomplete dictionary constructing and achieves a substantial low computational complexity.

3) we propose an efficient 2D-DOA and frequency estimation algorithm for L-shaped array which has close angle and frequency estimation performance compared with conventional PARAFAC method, and outperforms the ESPRIT algorithm in [8] and PM algorithm in [9].

The remainder of our paper is structured as follows: section II presents the received data model of multi-delay received signals for L-shaped array. Based on this model, section III derives the proposed CS-PARAFAC algorithm and section IV provides the CRB as well as the complexity analysis. Numerical simulations are exhibited in section V to demons- trate the performance of the proposed approach and we conclude this paper in section VI.

Notation: Matrices and vectors are represented by boldfaced capital letters and lower case letters respectively. $\otimes$, $\circ$ and $\oplus$ stand for *Kronecker* product, *Khatri–Rao* product and *Hadamard* product, respectively. $(.)^*$, $(.)^T$, $(.)^H$ and $(.)^{-1}$ denote the operations of complex conjugation, transpose, conjugate-transpose and inverse, respectively. $(\cdot)^\dagger$ denotes the Moore-Penrose pseudoinverse. $\|\cdot\|_F$ and $\|\cdot\|_0$ represent the *Forbenius* norm and l_0–norm. $D_n(\mathbf{A})$ denotes a diagonal matrix consisting of the$n$-th row of $\mathbf{A}$. $\mathbf{I}_M$ and $\mathbf{0}_M$ stand for a $M \times M$ identity matrix and zero matrix, respectively. $abs(.)$ stands for the modulus value symbol and $angle(.)$ is the phase angle operator. $Re(\cdot)$ and $Im(\cdot)$ represent the real part and imaginary part of a complex number.

II. DATA MODEL

Assume that there are K signals impinging on a L-shaped array which consists of two orthogonal M-element and N-element uniform linear arrays with inter-sensor spacing along x-axis and y-axis, respectively. The reference element is placed at the origin. The structure of the L-shaped array is shown in Fig.1. For the sensors on the x-axis, the distance between the m-th sensor and the reference element $(m = 1)$ is d_m^x, while for the y-axis, the distance between the n-th sensor and the reference element $(n = 1)$ is d_n^y.

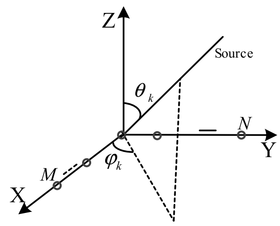

FIGURE 1. The structure of signal receiving array with L-shaped configuration.

Assume that the received noise is additive white Gaussian independent and uncorrelated with incident signals. The K signals are all uncorrelated narrow-band plane waves with different frequency. For the k-th signal, the real carrier frequency is f_k and the 2D-DOA is (φ_k, θ_k), where φ_k and θ_k are the azimuth angle and elevation angle, respectively. The received data of x-axis and y-axis subarrays at the t-th snapshot can be written as [27]

$$\mathbf{x}(t) = \mathbf{A}_x\mathbf{s}(t) + \mathbf{n}_x(t), \tag{1}$$

$$\mathbf{y}(t) = \mathbf{A}_y\mathbf{s}(t) + \mathbf{n}_y(t), \tag{2}$$

where $\mathbf{s}(t) = [s_1(t), s_2(t), \cdots, s_K(t)]^T$ is the K sources vector. $\mathbf{A}_x^{M\times K} = [\mathbf{a}_x(\varphi_1, \theta_1, f_1), \mathbf{a}_x(\varphi_2, \theta_2, f_2), \cdots, \mathbf{a}_x(\varphi_K, \theta_K, f_K)]$ is the x-axis subarray steering matrix with $\mathbf{a}_x(\varphi_k, \theta_k, f_k) = [1, \exp(-j2\pi d_2^x f_k \cos\varphi_k \sin\theta_k/c), \cdots, \exp(-j2\pi d_M^x f_k \cos\varphi_k \sin\theta_k/c)]^T$. $\mathbf{A}_y^{(N-1)\times K} = [\mathbf{a}_y(\varphi_1, \theta_1, f_1), \mathbf{a}_y(\varphi_2, \theta_2, f_2), \cdots, \mathbf{a}_y(\varphi_K, \theta_K, f_K)]$ is the steering matrix of the $N - 1$ sensors on y-axis (not including the reference element) with $\mathbf{a}_y(\varphi_k, \theta_k, f_k) = [\exp(-j2\pi d_2^y f_k \sin\varphi_k \sin\theta_k/c), \cdots, \exp(-j2\pi d_N^y f_k \sin\varphi_k \sin\theta_k/c)]^T$. c is the signal propagation velocity and $\mathbf{n}_x(t) \in \mathbf{C}^{M\times 1}$, $\mathbf{n}_y(t) \in \mathbf{C}^{(N-1)\times 1}$ are the received noise. Combining the received data matrix of two subarrays [28], [29]

$$\mathbf{z}_0(t) = \begin{bmatrix} \mathbf{x}(t) \\ \mathbf{y}(t) \end{bmatrix} = \mathbf{A}\mathbf{s}(t) + \mathbf{n}(t), \tag{3}$$

where $\mathbf{A} = \begin{bmatrix} \mathbf{A}_x \\ \mathbf{A}_y \end{bmatrix}$ is the two subarrays steering matrix and $\mathbf{n}(t) = \begin{bmatrix} \mathbf{n}_x(t) \\ \mathbf{n}_y(t) \end{bmatrix}$ is the noise of L-shaped array at t-th time.

To estimate the frequency, we introduce multi-delay outputs for the received signals. We consider $P-1$ delays where the delay time of the p-th delay is $\tau_p = p\tau$ and τ satisfies $0 < \tau < 1/[(P-1)\max(f_1, \ldots, f_K)]$ [9]. The structure of the multi- delay receiving array is shown in Fig. 2.

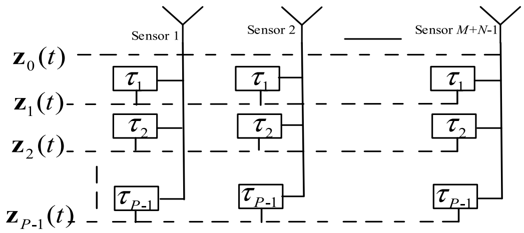

FIGURE 2. The received signals of multiple delay outputs [8].

For the p-th delay τ_p, the outputs data can be written as [9]

$$\begin{aligned} \mathbf{z}_p(t) &= \mathbf{z}_0(t - p\tau) \\ &= \mathbf{A}\mathbf{s}(t - p\tau) + \mathbf{n}(t - p\tau) \\ &= \mathbf{A}D_{p+1}(\mathbf{F})\mathbf{s}(t) + \mathbf{n}_p(t), \end{aligned} \tag{4}$$

where $\mathbf{n}_p(t) = \mathbf{n}(t - p\tau)$ is the noise of p-th delay outputs, and $\mathbf{F}^{P\times K}$ is the delay matrix defined by

$$\mathbf{F} \triangleq \begin{bmatrix} 1 & 1 & \cdots & 1 \\ e^{-j2\pi f_1 \tau} & e^{-j2\pi f_2 \tau} & \cdots & e^{-j2\pi f_K \tau} \\ \vdots & \vdots & \ddots & \vdots \\ e^{-j2\pi f_1 (P-1)\tau} & e^{-j2\pi f_2 (P-1)\tau} & \cdots & e^{-j2\pi f_K (P-1)\tau} \end{bmatrix}. \tag{5}$$

Then the p-th delay received data matrix with J snapshots is written as

$$\begin{aligned} \mathbf{Z}_p &= [\mathbf{z}_p(t_1), \mathbf{z}_p(t_2), \ldots, \mathbf{z}_p(t_J)] \\ &= \mathbf{A}D_{p+1}(\mathbf{F})\mathbf{S}^T + \mathbf{N}_p, \end{aligned} \tag{6}$$

where $\mathbf{S}^{J\times K} = [\mathbf{s}(t_1), \mathbf{s}(t_2), \ldots, \mathbf{s}(t_J)]^T$ and $\mathbf{N}_p = [\mathbf{n}_p(t_1), \mathbf{n}_p(t_2), \ldots, \mathbf{n}_p(t_J)]$. Stacking P delay outputs data into a new matrix, we obtain the received data [18]

$$\begin{aligned} \mathbf{Z}^{(M+N-1)P\times J} &= \begin{bmatrix} \mathbf{Z}_0 \\ \mathbf{Z}_1 \\ \vdots \\ \mathbf{Z}_{P-1} \end{bmatrix} = \begin{bmatrix} \mathbf{A}D_1(\mathbf{F}) \\ \mathbf{A}D_2(\mathbf{F}) \\ \vdots \\ \mathbf{A}D_P(\mathbf{F}) \end{bmatrix} \mathbf{S}^T + \begin{bmatrix} \mathbf{N}_0 \\ \mathbf{N}_1 \\ \vdots \\ \mathbf{N}_{P-1} \end{bmatrix} \\ &= [\mathbf{F} \circ \mathbf{A}]\mathbf{S}^T + \mathbf{N}, \end{aligned} \tag{7}$$

where $\mathbf{N} = [\mathbf{N}_0^T, \mathbf{N}_1^T, \ldots, \mathbf{N}_{P-1}^T]^T$.

III. JOINT 2D-DOA AND FREQUENCY ESTIMATION ALGORITHM

After obtaining the received data model (7), the traditional PARAFAC algorithm [18] usually performs the PARAFAC decomposition directly on (7) to get the estimations of angle and frequency. However, it suffers from a heavy computational load, especially when the number of sensors or snapshots are large. In order to resolve this drawback, [23] combines the compressed sensing theory with PARAFAC model and presents a joint angle and frequency estimation algorithm with linear array. However, it compresses the whole received data model directly and can only obtain one-dimensional DOA. In this paper, in order to reduce the complexity of traditional PARAFAC algorithm for L-shaped array and avoid construc- ting two-dimensional overcomplete dictionary for signal recovery, we make some changes of the compression process in [23] and compress the received data model in (7) with partitioning before performing the PARAFAC decomposition, then the 2D-DOA and frequency estimations can be obtained through sparse recovery.

A. COMPRESSION

In this subsection, we first take an elementary row transformation on the received data $\mathbf{Z}$ in (7) as

$$\mathbf{Z}_I = \mathbf{G}\mathbf{Z} = [\mathbf{A} \circ \mathbf{F}]\mathbf{S}^T + \mathbf{N}_I, \tag{8}$$

where $\mathbf{G} \in \mathbf{C}^{(M+N-1)P\times(M+N-1)P}$ is a transformation matrix corres- ponding to the finite number of row interchanged operations, and can be expressed as

$$\mathbf{G} = \left.\begin{bmatrix} \overbrace{1\,0\,\cdots\,0}^{M+N-1} & & & \\ & 1\,0\,\cdots\,0 & & \\ & & \ddots & \\ & & & 1\,0\,\cdots\,0 \\ 0\,1\,\cdots\,0 & & & \\ & 0\,1\,\cdots\,0 & & \\ & & \ddots & \\ & & & 0\,1\,\cdots\,0 \\ & & \vdots & \\ 0\,0\,\cdots\,1 & & & \\ & 0\,0\,\cdots\,1 & & \\ & & \ddots & \\ & & & 0\,0\,\cdots\,1 \end{bmatrix}\right. \begin{matrix} \left.\vphantom{\begin{matrix}1\\1\\1\\1\end{matrix}}\right\} P \\ \left.\vphantom{\begin{matrix}1\\1\\1\\1\end{matrix}}\right\} P \\ \\ \left.\vphantom{\begin{matrix}1\\1\\1\\1\end{matrix}}\right\} P \end{matrix}$$

$$\in \mathbf{C}^{(M+N-1)P\times(M+N-1)P}. \tag{9}$$

In noiseless case, the received data $\mathbf{Z}_I$ in (8) can be written as the PARAFAC model [15]

$$z_{m+n,j,p} = \sum_{k=1}^{K} \mathbf{F}(p,k)\mathbf{S}(j,k)\mathbf{A}(m+n,k),$$
$$m = 1, \ldots, M; \quad n = 1, \ldots, N-1;$$
$$j = 1, \ldots, J; \quad p = 1, \ldots, P, \tag{10}$$

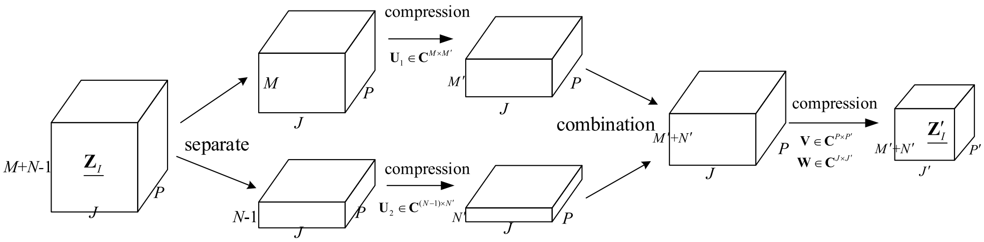

FIGURE 3. **The compression process.**

where $\mathbf{F}(p, k)$ is the (p, k) element of $\mathbf{F}$, $\mathbf{S}(j, k)$ is the (j, k) element of $\mathbf{S}$ and $\mathbf{A}(m + n, k)$ is the $(m + n, k)$ element of $\mathbf{A}$. The structure feature of the PARAFAC model in (10) indicates two other rearranged matrices [18]

$$\mathbf{Z}_{II} = [\mathbf{S} \circ \mathbf{A}]\mathbf{F}^T + \mathbf{N}_{II}, \tag{11}$$

$$\mathbf{Z}_{III} = [\mathbf{F} \circ \mathbf{S}]\mathbf{A}^T + \mathbf{N}_{III}. \tag{12}$$

Then, we compress the received data $\mathbf{Z}_I \in \mathbf{C}^{(M+N-1)\times J\times P}$ into a smaller matrix $\underline{\mathbf{Z}'_I} \in \mathbf{C}^{(M'+N')\times \overline{J'}\times P'}$, where $M < M'$, $N' < N-1$, $J' < J$ and $P' < P$. Fig.3 shows the compression process.

The four compression matrices $\mathbf{U}_1 \in \mathbf{C}^{M\times M'}(M' < M)$, $\mathbf{U}_2 \in \mathbf{C}^{(N-1)\times N'}(N' < N-1)$, $\mathbf{V} \in \mathbf{C}^{P\times P'}(P' < P)$ and $\mathbf{W} \in \mathbf{C}^{J\times J'}(J' < J)$, according to [30], should satisfy the restricted isometry property (RIP), and we can construct them through the Tucker3 decomposition [22] or random special matrices such as random Gaussian, Bernoulli or partial Fourier matrices [30].

The received data (8) can be divided into two parts as

$$\mathbf{Z}_I = \left[\begin{pmatrix}\mathbf{A}_x\\ \mathbf{A}_y\end{pmatrix} \circ \mathbf{F}\right]\mathbf{S}^T + \mathbf{N}_I = \begin{bmatrix}(\mathbf{A}_x \circ \mathbf{F})\mathbf{S}^T\\ (\mathbf{A}_y \circ \mathbf{F})\mathbf{S}^T\end{bmatrix} + \begin{bmatrix}\mathbf{N}_{Ix}\\ \mathbf{N}_{Iy}\end{bmatrix} = \begin{bmatrix}\mathbf{Z}_{Ix}\\ \mathbf{Z}_{Iy}\end{bmatrix} \tag{13}$$

where $\mathbf{Z}_{Ix} = (\mathbf{A}_x \circ \mathbf{F})\mathbf{S}^T + \mathbf{N}_{Ix}$ and $\mathbf{Z}_{Iy} = (\mathbf{A}_y \circ \mathbf{F})\mathbf{S}^T + \mathbf{N}_{Iy}$ are the received data of the array on x-axis and y-axis, respectively. Then the compressed receive data $\mathbf{Z}'_I \in \mathbf{C}^{(M'+N')J'\times P'}$ can be obtained by

$$\begin{aligned}
\mathbf{Z}'_I &= \begin{bmatrix}(\mathbf{U}_1^T \otimes \mathbf{V}^T)\mathbf{Z}_{Ix}\mathbf{W}\\ (\mathbf{U}_2^T \otimes \mathbf{V}^T)\mathbf{Z}_{Iy}\mathbf{W}\end{bmatrix}\\
&= \begin{bmatrix}(\mathbf{U}_1^T \otimes \mathbf{V}^T)(\mathbf{A}_x \circ \mathbf{F})\mathbf{S}^T\mathbf{W}\\ (\mathbf{U}_2^T \otimes \mathbf{V}^T)(\mathbf{A}_y \circ \mathbf{F})\mathbf{S}^T\mathbf{W}\end{bmatrix} + \begin{bmatrix}(\mathbf{U}_1^T \otimes \mathbf{V}^T)\mathbf{N}_{Ix}\mathbf{W}\\ (\mathbf{U}_2^T \otimes \mathbf{V}^T)\mathbf{N}_{Iy}\mathbf{W}\end{bmatrix}\\
&= \begin{bmatrix}(\mathbf{U}_1^T\mathbf{A}_x) \circ (\mathbf{V}^T\mathbf{F})\\ (\mathbf{U}_2^T\mathbf{A}_y) \circ (\mathbf{V}^T\mathbf{F})\end{bmatrix}(\mathbf{W}^T\mathbf{S})^T + \begin{bmatrix}(\mathbf{U}_1^T \otimes \mathbf{V}^T)\mathbf{N}_{Ix}\mathbf{W}\\ (\mathbf{U}_2^T \otimes \mathbf{V}^T)\mathbf{N}_{Iy}\mathbf{W}\end{bmatrix}\\
&= \left[\begin{pmatrix}\mathbf{U}_1^T\mathbf{A}_x\\ \mathbf{U}_2^T\mathbf{A}_y\end{pmatrix} \circ \mathbf{V}^T\mathbf{F}\right](\mathbf{W}^T\mathbf{S})^T + \mathbf{N}'_I\\
&= [\mathbf{A}' \circ \mathbf{F}']\mathbf{S}'^T + \mathbf{N}'_I,
\end{aligned} \tag{14}$$

where $\mathbf{A}' = \begin{bmatrix}\mathbf{U}_1^T\mathbf{A}_x\\ \mathbf{U}_2^T\mathbf{A}_y\end{bmatrix}$, $\mathbf{F}' = \mathbf{V}^T\mathbf{F}$ and $\mathbf{S}' = \mathbf{W}^T\mathbf{S}$. $\mathbf{N}'_I$ is the compressed noise.

The compressed received data $\mathbf{Z}'_I$ also can be expressed as the PARAFAC model, and according to (11) and (12), we can obtain two other arranged matrices

$$\mathbf{Z}'_{II} = [\mathbf{S}' \circ \mathbf{A}']\mathbf{F}'^T + \mathbf{N}'_{II}, \tag{15}$$

$$\mathbf{Z}'_{III} = [\mathbf{F}' \circ \mathbf{S}']\mathbf{A}'^T + \mathbf{N}'_{III}, \tag{16}$$

where $\mathbf{N}'_{II}$ and $\mathbf{N}'_{III}$ are the noise after compression.

B. PARAFAC DECOMPOSITION

TALS algorithm is a common method for the decomposition of PARAFAC model [31]. And the basic idea of TALS algorithm is to update one matrix in the PARAFAC model each time until convergence. The detailed derivation is shown as follows.

According to (14), the LS fitting is

$$\min_{\mathbf{A}',\mathbf{F}',\mathbf{S}'} \left\|\mathbf{Z}'_I - [\mathbf{A}' \circ \mathbf{F}']\mathbf{S}'^T\right\|_F, \tag{17}$$

then the LS update for $\mathbf{S}'$ is

$$\hat{\mathbf{S}}'^T = [\hat{\mathbf{A}}' \circ \hat{\mathbf{F}}']^\dagger \mathbf{Z}'_I, \tag{18}$$

where $\hat{\mathbf{A}}'$ and $\hat{\mathbf{F}}'$ are the previous estimates of $\mathbf{F}'$ and $\mathbf{A}'$, respectively.

Similarly, according to (15), the LS fitting is

$$\min_{\mathbf{A}',\mathbf{F}',\mathbf{S}'} \left\|\mathbf{Z}'_{II} - [\mathbf{S}' \circ \mathbf{A}']\mathbf{F}'^T\right\|_F, \tag{19}$$

then the LS update for $\mathbf{F}'$ is

$$\hat{\mathbf{F}}'^T = [\hat{\mathbf{S}}' \circ \hat{\mathbf{A}}']^\dagger \mathbf{Z}'_{II}, \tag{20}$$

where $\hat{\mathbf{A}}'$ and $\hat{\mathbf{S}}'$ are the previous estimates of $\mathbf{A}'$ and $\mathbf{S}'$, respectively.

And from (16), the LS fitting amounts to

$$\min_{\mathbf{A}',\mathbf{F}',\mathbf{S}'} \left\|\mathbf{Z}'_{III} - [\mathbf{F}' \circ \mathbf{S}']\mathbf{A}'^T\right\|_F, \tag{21}$$

then the LS update for $\mathbf{A}'$ is

$$\hat{\mathbf{A}}'^T = [\hat{\mathbf{F}}' \circ \hat{\mathbf{S}}']^\dagger \mathbf{Z}'_{III}, \tag{22}$$

where $\hat{\mathbf{F}}'$ and $\hat{\mathbf{S}}'$ are the previous estimates of $\mathbf{F}'$ and $\mathbf{S}'$, respectively.

Now, we have demonstrated the derivation of TALS algorithm for the decomposition of PARAFAC model above. Define $\mathbf{E} = \mathbf{Z}'_I - [\hat{\mathbf{A}}' \circ \hat{\mathbf{F}}']\hat{\mathbf{S}}'^T$ as the estimation error of the received data, where $\hat{\mathbf{A}}'$, $\hat{\mathbf{F}}'$ and $\hat{\mathbf{S}}'$ stand for the estimates of $\mathbf{A}'$, $\mathbf{F}'$ and $\mathbf{S}'$, respectively. Define $SSR = \sum_{j=1}^{J'}\sum_{i=1}^{(M'+N')P'}\left|e_{ij}\right|^2$ to be the sum of squared residuals (SSR) in PARAFAC decomposition, where e_{ij} stands for the (i,j) element of $\mathbf{E}$. According to (18), (20) and (22), we repeatedly update the estimation matrices $\hat{\mathbf{S}}'$, $\hat{\mathbf{F}}'$ and $\hat{\mathbf{A}}'$ until SSR less than a certain pimping value. Ultimately, we acquire the final estimates of $\mathbf{S}'$, $\mathbf{F}'$ and $\mathbf{A}'$.

Theorem 1 [32]: For $\mathbf{Z}'_I = [\mathbf{A}' \circ \mathbf{F}']\mathbf{S}'^T$, where $\mathbf{A}' \in \mathbf{C}^{(M'+N')\times K}$, $\mathbf{F}' \in \mathbf{C}^{P'\times K}$ and $\mathbf{S}' \in \mathbf{C}^{J'\times K}$, if

$$k_{\mathbf{A}'} + k_{\mathbf{S}'} + k_{\mathbf{F}'} \geq 2K + 2, \tag{23}$$

where $k_{\mathbf{A}'}$, $k_{\mathbf{S}'}$ and $k_{\mathbf{F}'}$ are the k-rank [14] of $\mathbf{A}'$, $\mathbf{S}'$ and $\mathbf{F}'$, respectively, then $\mathbf{A}'$, $\mathbf{S}'$ and $\mathbf{F}'$ are unique if taking no account of the permutation and scaling of columns.

Utilizing the PARAFAC decomposition, finally we can obtain the estimates of $\mathbf{F}'$, $\mathbf{A}'$ and $\mathbf{S}'$ as

$$\hat{\mathbf{F}}' = \mathbf{F}'\mathbf{\Pi}\mathbf{\Delta}_1 + \mathbf{W}_1, \tag{24}$$
$$\hat{\mathbf{A}}' = \mathbf{A}'\mathbf{\Pi}\mathbf{\Delta}_2 + \mathbf{W}_2, \tag{25}$$
$$\hat{\mathbf{S}}' = \mathbf{S}'\mathbf{\Pi}\mathbf{\Delta}_3 + \mathbf{W}_3, \tag{26}$$

where $\mathbf{\Pi}$ stands for the permutation matrix, $\mathbf{\Delta}_1$, $\mathbf{\Delta}_2$ and $\mathbf{\Delta}_3$ are the diagonal scaling matrices which satisfy $\mathbf{\Delta}_1\mathbf{\Delta}_2\mathbf{\Delta}_3 = \mathbf{I}$. $\mathbf{W}_1$, $\mathbf{W}_2$ and $\mathbf{W}_3$ are the estimation errors. We can eliminate scale ambiguity by normalization effortlessly and as for the permutation ambiguity, it makes no difference for the angle and frequency estimation of our proposed algorithm.

C. 2D-DOA AND FREQUENCY ESTIMATION WITH SPARSITY

Till now, we have gained the estimates of $\mathbf{A}'$ and $\mathbf{F}'$ via PARAFAC decomposition, and the estimations of 2D-DOA and frequency can be obtained from the compressed matrices $\hat{\mathbf{A}}'$ and $\hat{\mathbf{F}}'$ with sparsity.

1) FREQUENCY ESTIMATION

Denote the k-th column of $\hat{\mathbf{F}}'$ as $\hat{\mathbf{f}}'_k$, then as $\mathbf{F}' = \mathbf{V}^T\mathbf{F}$ and according to (24), we have

$$\hat{\mathbf{f}}'_k = \mathbf{V}^T\partial_{fk}\mathbf{f}_k + \mathbf{w}_{1k}, \tag{27}$$

where $\mathbf{f}_k$ is the k-th column of $\mathbf{F}$ and $\mathbf{w}_{1k}$ is the estimation error, ∂_{fk} is the scaling coefficient. Let $\{\tilde{f}_1, \tilde{f}_2, \ldots, \tilde{f}_r, \ldots, \tilde{f}_R\}$be a sampling grid of all possible frequency, where $R \gg K$. Then we construct a Vandermonde matrix $\tilde{\mathbf{F}}^{P\times R} = [\tilde{\mathbf{f}}_1, \cdots, \tilde{\mathbf{f}}_r, \cdots, \tilde{\mathbf{f}}_R]$ with $\tilde{\mathbf{f}}_r = [1, \exp(-j2\pi\tilde{f}_r\tau), \ldots, \exp(-j2\pi\tilde{f}_r(P-1)\tau)]^T$. $\tilde{\mathbf{F}}$ can be regarded as a overcomplete dictionary for the frequency estimation, and if there have $f_k = \tilde{f}_r$, then there exist a sparse vector $\mathbf{e}_r \in \mathbf{C}^{R\times 1}$, the r-th element of which is one and the others are zero, that satisfies $\mathbf{f}_k = \tilde{\mathbf{F}}e_r$. Then (27) can be converted to

$$\hat{\mathbf{f}}'_k = \mathbf{V}^T\partial_{fk}\tilde{\mathbf{F}}e_r + \mathbf{w}_{1k}. \tag{28}$$

The estimate of $\mathbf{e}_r$ can be obtained via l_0-norm constraint [23]

$$\min_{\mathbf{e}_r}\left\|\hat{\mathbf{f}}'_k - \mathbf{V}^T\partial_{fk}\tilde{\mathbf{F}}e_r\right\|_F^2, \quad s.t.\ \|\mathbf{e}_r\|_0 = 1. \tag{29}$$

(29) can be further simplified to

$$\min_{\tilde{f}_r}\left\|\hat{\mathbf{f}}'_k - \mathbf{V}^T\tilde{\mathbf{f}}_r\partial_{fk}\right\|_F^2. \tag{30}$$

According to (27), we can get the estimation of $\partial_{fk} = (\mathbf{V}^T\tilde{\mathbf{f}}_r)^{\dagger}\hat{\mathbf{f}}'_k$, then the estimates of f_k can be obtained via

$$\hat{f}_k = \min_{\tilde{f}_r}\left\|\hat{\mathbf{f}}'_k - \mathbf{V}^T\tilde{\mathbf{f}}_r(\mathbf{V}^T\tilde{\mathbf{f}}_r)^{+}\hat{\mathbf{f}}'_k\right\|_F^2,$$
$$r = 1, 2, \ldots, R, \quad k = 1, 2, \ldots, K. \tag{31}$$

2) 2D-DOA ESTIMATION

According to (14) and (25), we have

$$\begin{aligned}\hat{\mathbf{A}}' &= \mathbf{A}'\Pi\Delta_2 + \mathbf{W}_2 = \begin{bmatrix}\mathbf{U}_1^T\mathbf{A}_x\\ \mathbf{U}_2^T\mathbf{A}_y\end{bmatrix}\mathbf{\Pi}\mathbf{\Delta}_2 + \mathbf{W}_2\\ &= \begin{bmatrix}\mathbf{U}_1^T\mathbf{A}_x\mathbf{\Pi}\mathbf{\Delta}_2 + \mathbf{W}_{2x}\\ \mathbf{U}_2^T\mathbf{A}_y\mathbf{\Pi}\mathbf{\Delta}_2 + \mathbf{W}_{2y}\end{bmatrix} = \begin{bmatrix}\hat{\mathbf{A}}'_x\\ \hat{\mathbf{A}}'_y\end{bmatrix},\end{aligned} \tag{32}$$

where $\hat{\mathbf{A}}'_x = \mathbf{U}_1^T\mathbf{A}_x\mathbf{\Pi}\mathbf{\Delta}_2 + \mathbf{W}_{2x}$ is the first M' rows of $\hat{\mathbf{A}}'$ and $\hat{\mathbf{A}}'_y = \mathbf{U}_2^T\mathbf{A}_y\mathbf{\Pi}\mathbf{\Delta}_2 + \mathbf{W}_{2y}$ is the last N' rows of $\hat{\mathbf{A}}'$. Denote the k-th column of $\hat{\mathbf{A}}'_x$ and $\hat{\mathbf{A}}'_y$ as $\hat{\mathbf{a}}'_{xk}$ and $\hat{\mathbf{a}}'_{yk}$, respectively, then we have

$$\hat{\mathbf{a}}'_{xk} = \mathbf{U}_1^T\partial_{xk}\mathbf{a}_{xk} + \mathbf{w}_{2xk}, \tag{33}$$
$$\hat{\mathbf{a}}'_{yk} = \mathbf{U}_2^T\partial_{yk}\mathbf{a}_{yk} + \mathbf{w}_{2yk}, \tag{34}$$

where $\mathbf{a}_{xk}$ and $\mathbf{a}_{yk}$ is the k-th column of $\mathbf{A}_x$ and $\mathbf{A}_y$, respectively. $\mathbf{w}_{2xk}$ and $\mathbf{w}_{2yk}$ are the corresponding estimation error, ∂_{xk} and ∂_{yk} are the scaling coefficients.

Define $u_k \cos\varphi_k \sin\theta_k$ and $v_k \sin\varphi_k \sin\theta_k$. Let $\{\tilde{u}_1, \tilde{u}_2, \ldots, \tilde{u}_g, \ldots, \tilde{u}_G\}$ and $\{\tilde{v}_1, \tilde{v}_2, \ldots, \tilde{v}_q, \ldots, \tilde{v}_Q\}$ be a sampling grid of all potential sources location, where $G \gg K$ and $Q \gg K$. Constructing two Vandermonde matrices $\tilde{\mathbf{A}}_{xk}^{M\times G} = [\tilde{\mathbf{a}}_{xk1}, \cdots, \tilde{\mathbf{a}}_{xkg}, \cdots, \tilde{\mathbf{a}}_{xkG}]$ and $\tilde{\mathbf{A}}_{yk}^{(N-1)\times Q} = [\tilde{\mathbf{a}}_{yk1}, \cdots, \tilde{\mathbf{a}}_{ykq}, \cdots, \tilde{\mathbf{a}}_{ykQ}]$, where $\tilde{\mathbf{a}}_{xkg} = [1, \exp(-j2\pi d_2^x\hat{f}_k\tilde{u}_g/c), \cdots, \exp(-j2\pi d_M^x\hat{f}_k\tilde{u}_g/c)]^T$ and $\tilde{\mathbf{a}}_{ykq} = [\exp(-j2\pi d_2^y\hat{f}_k\tilde{v}_q/c), \cdots, \exp(-j2\pi d_N^y\hat{f}_k\tilde{v}_q/c)]^T$. $\tilde{\mathbf{A}}_{xk}$ and $\tilde{\mathbf{A}}_{yk}$ can be regarded as the overcomplete dictionary for the angle estimations, and when $u_k = \tilde{u}_g$, $v_k = \tilde{v}_q$, there exist two sparse vectors $\mathbf{e}_g \in \mathbf{C}^{G\times 1}$ and $\mathbf{e}_q \in \mathbf{C}^{Q\times 1}$ that satisfy $\mathbf{a}_{xk} = \tilde{\mathbf{A}}_{xk}\mathbf{e}_g$ and $\mathbf{a}_{yk} = \tilde{\mathbf{A}}_{yk}\mathbf{e}_q$, respectively. Then (33) and (34) can be converted to

$$\hat{\mathbf{a}}'_{xk} = \mathbf{U}_1^T\partial_{xk}\tilde{\mathbf{A}}_{xk}\mathbf{e}_g + \mathbf{w}_{2xk}, \tag{35}$$
$$\hat{\mathbf{a}}'_{yk} = \mathbf{U}_2^T\partial_{yk}\tilde{\mathbf{A}}_{yk}\mathbf{e}_q + \mathbf{w}_{2yk}. \tag{36}$$

Now, similarly, the estimates of u_k and v_k can be obtained by l_0-norm constraint as

$$\hat{u}_k = \min_{\tilde{u}_g}\left\|\hat{\mathbf{a}}'_{xk} - \mathbf{U}_1^T\tilde{\mathbf{a}}_{xkg}(\mathbf{U}_1^T\tilde{\mathbf{a}}_{xkg})^{+}\hat{\mathbf{a}}'_{xk}\right\|_F^2,$$
$$g = 1, 2, \ldots, G,\ k = 1, 2, \ldots, K. \tag{37}$$

$$\hat{v}_k = \min_{\tilde{v}_q} \left\| \hat{\mathbf{a}}'_{yk} - \mathbf{U}_2^T \tilde{\mathbf{a}}_{ykq} (\mathbf{U}_2^T \tilde{\mathbf{a}}_{ykq})^+ \hat{\mathbf{a}}'_{yk} \right\|_F^2, \quad q = 1, 2, \ldots, Q, \; k = 1, 2, \ldots, K. \tag{38}$$

Finally, we can get the estimates of θ_k and φ_k via

$$\hat{\theta}_k = \sin^{-1}(abs(\hat{u}_k + j\hat{v}_k)) \quad k = 1, 2, \ldots, K, \tag{39}$$

$$\hat{\varphi}_k = angle(\hat{u}_k + j\hat{v}_k) \quad k = 1, 2, \ldots, K, \tag{40}$$

where $\sin^{-1}(\cdot)$ is the arcsin function.

Remark 1: the estimates of elevation angles, azimuth angles and frequency also achieve paired automatically, due to the columns of the estimated compressed direction matrix and delay matrix automatically paired after PARAFAC decomposition.

Remark 2: In this paper, as a prior assumption, the sources number K is known, which can be attained by matrix decomposition method or information theory [33].

Remark 3: The off-grid problem will arise if the signals are not exactly located at the pre-defined grid points, which will sap the performance of CS methods and it can be solved via some self-adaption method like adaptive matching pursuit with constrained total least squares (AMP-CTLS) [34]. In this paper, we suppose that the grid for the angle and frequency space are densely enough and sufficient fine, the sources indeed fall on the 2D-DOA angles and frequency grids, so we do not consider the off-grid problem.

D. THE PROCEDURE OF THE PROPOSED ALGORITHM

Since, we have acquired the 2D-DOA and frequency estimations of received signals for L-shaped array and the major procedure can be summarized as follows:

Step 1: According to (8), transform the received data $\mathbf{Z}$ to $\mathbf{Z}_I$, then compress it into a small matrix $\mathbf{Z}'_I$ and obtain two other arranged matrices $\mathbf{Z}'_{II}$ and $\mathbf{Z}'_{III}$.

Step 2 : Initialize the value of $\mathbf{S}'$, $\mathbf{F}'$ and $\mathbf{A}'$ with Gaussian random matrix, then according to (18), (20) and (22), update the estimates of $\mathbf{S}'$, $\mathbf{F}'$ and $\mathbf{A}'$ repeatedly until *SSR* is less-than a certain tiny value.

Step 3: Construct the overcomplete dictionary of frequency and obtain the estimates of $\hat{f}_k$ $(k = 1, \ldots, K)$ via (31).

Step 4: Utilize $\hat{f}_k$ and according to (37)-(40), obtain the estimates of elevation angles and azimuth angles.

IV. PERFORMANCE ANALYSIS

In this part, we analyze the computational complexity of the proposed algorithm and present the derivation of the CRB, as well as the advantages of the proposed algorithm.

A. COMPLEXITY ANALYSIS

For the proposed CS-PARAFAC algorithm in this paper, the complexity of the compression process is $O[P'(M' + N')\, P(M + N - 1)J + JP'(M' + N')J']$. The complexity for each iteration is $O[3K^2 + K^2(J' + M' + N' + P') + 6K^2((M' + N')(P' + J') + J'P') + 3K(M' + N')J'P']$ and the complexity for signal sparse recovery is $O[K(MG + Q(N - 1) + PR)]$ [23]. So the whole complexity of the proposed algorithm is $O[P'(M' + N')\, P(M + N - 1)J + JP'(M' + N')J' + n_1(3K^2 + K^2(J' + M' + N' + P') + 6K^2((M' + N')(P' + J') + J'P') + 3K(M' + N')J'P') + K(MG + Q(N - 1) + PR)]$, where n_1 is the number of iterations. While for the traditional PARAFAC algorithm [18], the complexity is $O(n_2(3K^2 + K^2(J + M + N - 1 + P) + 6K^2((M + N - 1)(P + J) + JP) + 3K(M + N - 1)JP) + 2K^2(M + N - 1 + P) + 9K^3)$ [23], where n_2 is the number of iterations. To make a clear complexity comparison of these two algorithms, we consider $M = N = P = 10$ and $K = 3$. The number of iterations of these two methods are about dozens and we set $n_1 = n_2 = 30$ and assume that $G = Q = 200$, $R = 300$ and $M'/M = N'/N = J'/J = 0.5$. Fig. 4 shows the complexity comparison versus different snapshots J, and we can conclude that our proposed algorithm owns much lower computational load than traditional PARAFAC algorithm.

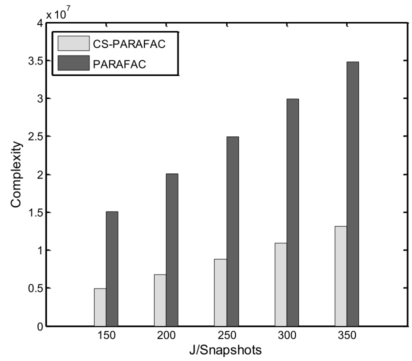

FIGURE 4. complexity comparison versus different snapshots (*J*).

B. CRAMER-RAO BOUND

In this subsection, we derive the CRB of the 2D-DOA and frequency estimations for L-shaped array. Define

$$\mathbf{B} = \mathbf{F} \circ \mathbf{A}. \tag{41}$$

Then according to [23]–[26], the CRB matrix can be represented by

$$\text{CRB} = \frac{\sigma^2}{2J} \left\{ \text{Re} \left[\mathbf{D}^H \mathbf{\Pi}_{\mathbf{B}}^{\perp} \mathbf{D} \oplus \mathbf{P}^T \right] \right\}^{-1}, \tag{42}$$

where $\mathbf{D} = \left[\frac{\partial \mathbf{b}_1}{\partial \varphi_1}, \ldots, \frac{\partial \mathbf{b}_K}{\partial \varphi_K}, \frac{\partial \mathbf{b}_1}{\partial \theta_1}, \ldots, \frac{\partial \mathbf{b}_K}{\partial \theta_K}, \frac{\partial \mathbf{b}_1}{\partial f_1}, \ldots, \frac{\partial \mathbf{b}_K}{\partial f_K} \right]$, $\mathbf{b}_k$ is the k-th column of $\mathbf{B}$. $\mathbf{\Pi}_{\mathbf{B}}^{\perp} = \mathbf{I} - \mathbf{B}\left(\mathbf{B}^H\mathbf{B}\right)^{-1}\mathbf{B}^H$, $\mathbf{P} = \mathbf{1}_{3\times 3} \otimes \mathbf{P}_s$ where $\mathbf{1}_{3\times 3}$ is a 3×3 matrix with all elements being one and $\hat{\mathbf{P}}_s = \frac{1}{J}\sum_{t=1}^{J} \mathbf{s}(t)\mathbf{s}^H(t)$.

C. ADVANTAGES OF THE PROPOSED ALGORITHM

The advantages of the proposed algorithm, parts of which are verified in section V, can be summarized as follows:

1) The proposed algorithm brings much lower computational complexity and need smaller data storage capacity, owing to its combination of PARAFAC model and compressed sensing theory.

2) The proposed algorithm is resultful for joint 2D-DOA and frequency estimation and is effective for both uniform and non-uniform L-shaped array, while the ESPRIT algorithm in [8] and PM algorithm in [9] are only resultful for uniform array.

3) The proposed algorithm can achieve paired elevation angles, azimuth angles and frequency automatically.

4) The 2D-DOA and frequency estimation performance of our algorithm is close to the traditional PARAFAC method [18], and better than that of ESPRIT algorithm in [8] and PM algorithm in [9].

V. SIMULATION RESULTS

We assume that there are three far-field incoherent sources impinge on a L-shaped array, the 2D-DOA and frequency of the sources are $(\varphi_1, \theta_1, f_1) = (10°, 15°, 1\text{MHz})$, $(\varphi_2, \theta_2, f_2) = (20°, 25°, 2\text{MHz})$ and $(\varphi_3, \theta_3, f_3) = (30°, 35°, 3\text{MHz})$, respectively. J is the snapshots and P is the number of delays. M and N are the sensor numbers of x-axis and y-axis, respectively. In the following simulations, the propagation speed of the signals are $c = 3 \times 10^8 m/s$ and the sampling rate is twice of the biggest frequency of the frequency grid. The compression matrices are obtained via random Gaussian matrix, as well as the initialization of the PARAFAC model. we employ the root mean square error (RMSE) to assess the 2D-DOA and frequency estimation performance of our proposed algorithm and define RMSE as

$$RMSE_{DOA} = \frac{1}{K}\sum_{k=1}^{K}\sqrt{\frac{1}{L}\sum_{l=1}^{L}[(\hat{\varphi}_{k,l}-\varphi_k)^2+(\hat{\theta}_{k,l}-\theta_k)^2]}, \tag{43}$$

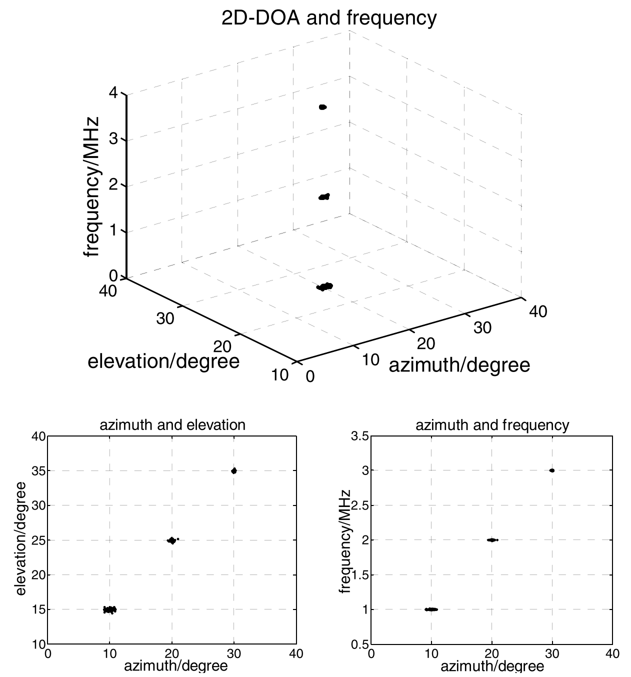

FIGURE 5. Angle and frequency estimation for uniform L-shaped array.

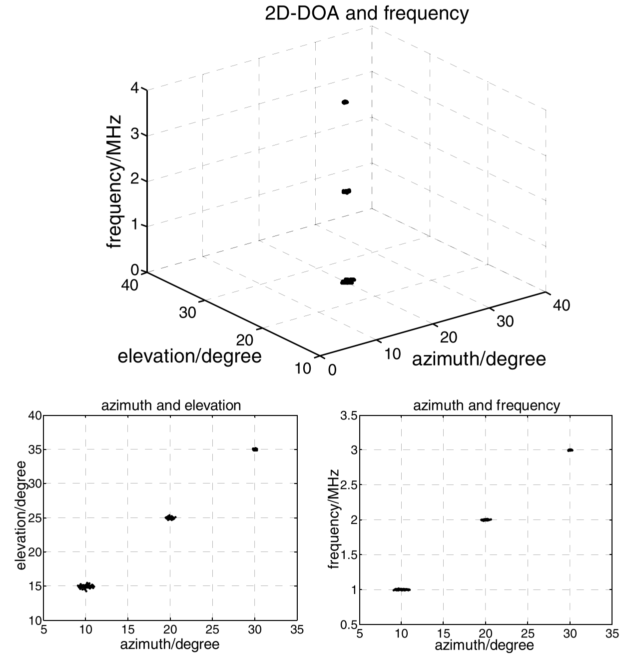

FIGURE 6. Angle and frequency estimation for non-uniform L-shaped array.

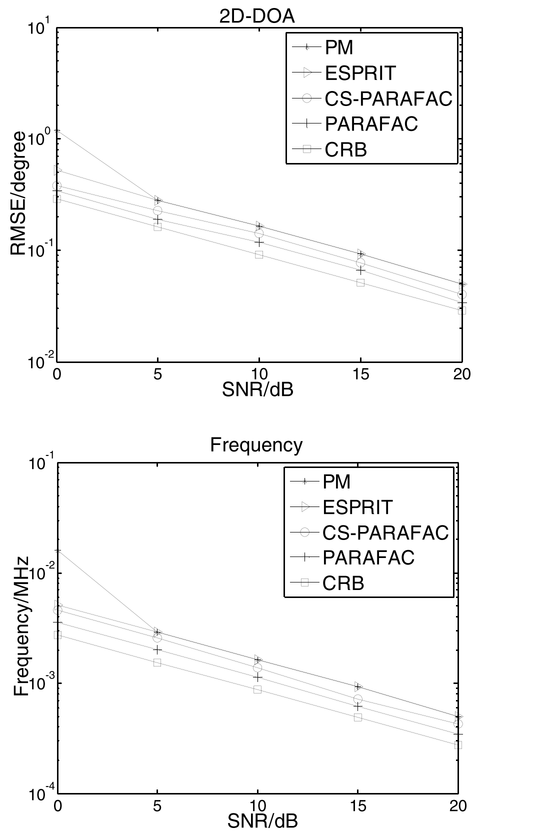

FIGURE 7. 2D-DOA and frequency estimation performance comparison.

$$RMSE_{frequency} = \frac{1}{K}\sum_{k=1}^{K}\sqrt{\frac{1}{L}\sum_{l=1}^{L}(\hat{f}_{k,l}-f_k)^2}, \tag{44}$$

where φ_k, θ_k and f_k are the precise elevation angle, azimuth angle and frequency of the k-th source, respectively.

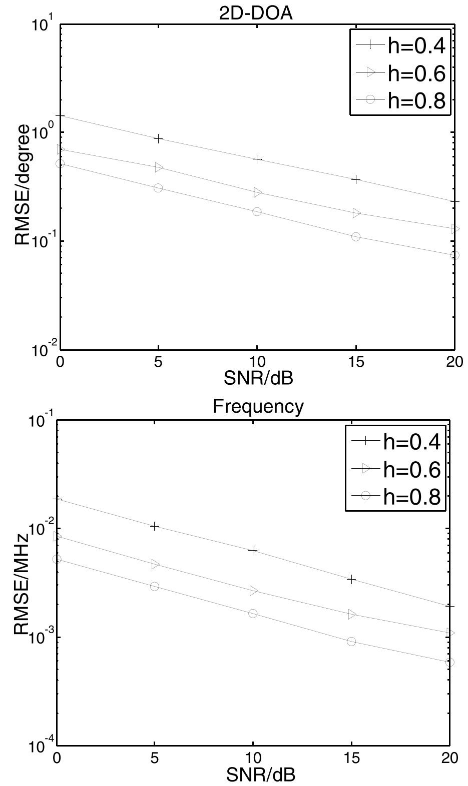

FIGURE 8. Angle and frequency estimation performance under different *h*.

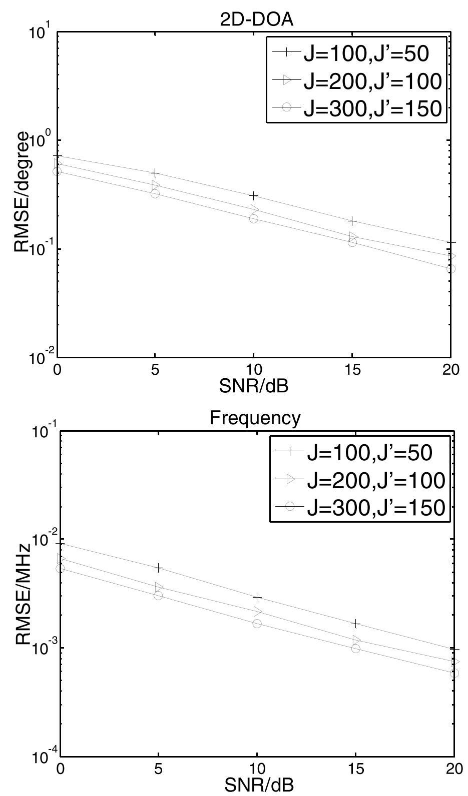

FIGURE 9. Angle and frequency estimation performance under different *J*.

$\hat{\varphi}_{k,l}$, $\hat{\theta}_{k,l}$, $\hat{f}_{k,l}$ are the estimates of φ_k, θ_k and f_k in l-th simulation. L indicates the total times of Monte-Carlo simulation trials and we set $L = 1000$ in this paper.

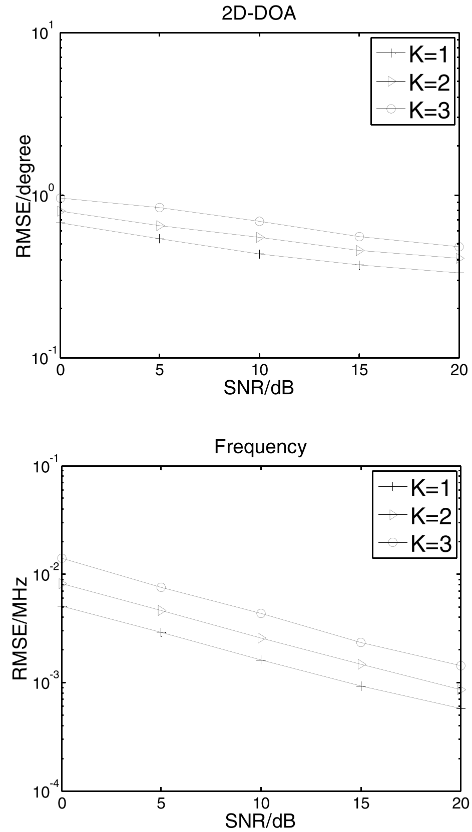

FIGURE 10. Angle and frequency estimation performance under different *K*.

Simulation 1: Fig. 5 and Fig. 6 show the 2D-DOA and frequency estimation results of our proposed algorithm with SNR=10dB. Define the size of PARAFAC model as $(M + N - 1) \times P \times J$. In simulation 1, the initial size of the received data is $(10 + 10 - 1) \times 10 \times 200$, which becomes $(5 + 5) \times 5 \times 100 \quad ((M' + N') \times P' \times J')$ after compression. Fig. 5 is the simulation result of uniform L-shaped array and the distance between every adjacent sensor is $d = 50m$. While in Fig. 6, the array is non-uniform and the distance between every sensor and the reference element are $d^x = [0, 60, 100, 162, 190, 265, 298, 364, 410, 450]$ and $d^y = [0, 50, 95, 150, 210, 256, 294, 360, 410, 455]$. We can conclude from Fig. 5 and Fig. 6 that our algorithm is efficient for both uniform and non-uniform L-shaped array.

Simulation 2: Fig.7 depicts the angle and frequency estimation performance comparison of our proposed algorithm, traditional PARAFAC algorithm [18], ESPRIT algorithm [8] and PM algorithm [9]. The original size of the receive data is $(10 + 10 - 1) \times 10 \times 200$,which is compressed into $(8 + 8) \times 8 \times 160$ in this simulation. Fig.7 manifests that the performance of our proposed algorithm is close to the traditional PARAFAC algorithm, and outperforms ESPRIT and PM algorithm.

Simulation 3: Fig.8 presents the 2D-DOA and frequency estimation performance of our proposed algorithm under different compression ratio. The compression ratio is defined as $h = M'/M = N'/N = J'/J = P'/P$. In simulation 3, the original PARAFAC model size is $(10 + 10 - 1) \times 10 \times 200$ with $h = 0.4$, $h = 0.6$ and $h = 0.8$, respectively. Fig.8 indicates that the 2D-DOA and frequency estimation performance of our approach improves when h gets larger.

Simulation 4: Fig.9 shows the 2D-DOA and frequency estimation performance of our proposed algorithm versus different snapshots (J). In this simulation, the size of the rectangular array is $M = 10$, $N = 10$ and $P = 10$, set the snapshots $J = 100$, $J = 200$ and$J = 300$, respectively. Assume that $M' = N' = P' = 8$ and $J'/J = 0.5$. Fig.9 demonstrates that the angle and frequency estimation performance of our approach gets better with the increase of snapshots (J).

Simulation 5: Fig.10 illustrates the angle and frequency estimation performance of our proposed algorithm with different source numbers. In simulation 5, fix $M = N = P = 10$, $J = 200$ and $N' = M' = P' = 5$, $J' = 100$. Set $K = 1$, $K = 2$ and $K = 3$, respectively. Fig.10 attests that the angle and frequency estimation performance of our approach will get worse for larger number of received sources.

Simulation 6: Fig.11 presents the 2D-DOA and frequency estimation performance of our proposed algorithm of different number of delays. In simulation 6, $M = N = 10$ and $M'/M = N'/N = 0.8$, $J = 200$ and $J' = 100$. Set $P = 6$, $P = 10$ and $P = 14$ with $P'/P = 0.5$, respectively.

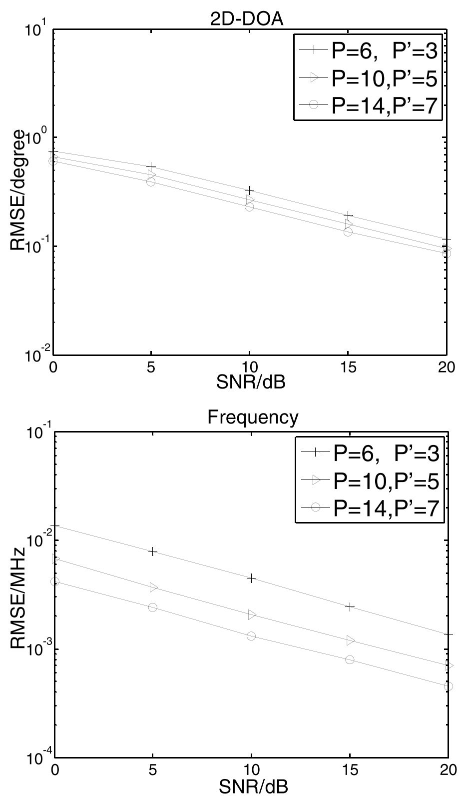

FIGURE 11. Angle and frequency estimation performance under different *P*.

Fig.11 indicates that the angle and frequency estimation performance of our approach improves with the increase of P. In addition, as we obtain the frequency estimation from the delay matrix, P shows bigger influence on the frequency estimation than angle estimation. If we want more accurate frequency estimation, it's better to choose a larger value for P.

VI. CONCLUSIONS

In this paper, we have combined the compressed sensing theory with the PARAFAC model to propose an effective 2D-DOA and frequency estimation algorithm for L-shaped array. The proposed method could obtain the automatically paired 2D-DOA and frequency estimation and owing to the compression, it exhibited smaller computational complexity remarkably as well as smaller demand for storage capacity, compared with traditional PARAFAC algorithm. The simulation results verified that the angle and frequency estimation performance of our approach was close to the traditional PARAFAC algorithm, and better than ESPRIT algorithm and PM algorithm.

REFERENCES

[1] H. Y. Kang, Y. S. Kim, and C. J. Kim, "Spatially close signals separation via array aperture expansions and spatial spectrum averaging," *ETRI J.*, vol. 26, no. 1, pp. 45–47, 2004.
[2] R. Rajagopal and P. R. Rao, "Generalised algorithm for DOA estimation in a passive sonar," *IEE Proc. F Radar Signal Process.*, vol. 140, no. 1, pp. 12–20, Feb. 1993.
[3] F. Belfiori, "Antenna array signal processing for multistatic radar systems," Delft Univ. Technol., Delft, The Netherlands, 2013.
[4] X. Huang *et al.*, "Adaptive beamforming for array signal processing in aeroacoustic measurements," *J. Acoust. Soc. Amer.*, vol. 131, no. 3, p. 2152, 2012.
[5] R. O. Schmidt, "Multiple emitter location and signal parameter estimation," *IEEE Trans. Antennas Propag.*, vol. AP-34, no. 3, pp. 276–280, Mar. 1986.
[6] J.-D. Lin, W.-H. Fang, Y.-Y. Wang, and J.-T. Chen, "FSF MUSIC for joint DOA and frequency estimation and its performance analysis," *IEEE Trans. Signal Process.*, vol. 54, no. 12, pp. 4529–4542, Dec. 2006.
[7] X. Wang, "Joint angle and frequency estimation using multiple-delay output based on ESPRIT," *EURASIP J. Adv. Signal Process.*, vol. 2010, Dec. 2010, Art. no. 358659.
[8] X. Wang, X. Zhang, J. Li, and J. Bai, "Improved ESPRIT method for joint direction-of-arrival and frequency estimation using multiple-delay output," *Int. J. Antennas Propag.*, vol. 2012, Jul. 2012, Art. no. 309269.
[9] Z. Sun, J. F. Li, J. Liu, and X. F. Zhang, "Propagator method-based joint angle and frequency estimation using multiple delay output," *ICIC Express Lett.*, vol. 2, no. 4, pp. 827–832, 2011.
[10] M. Haardt and J. A. Nossek, "3-D unitary ESPRIT for joint 2-D angle and carrier estimation," in *Proc. IEEE Int. Conf. Acoust., Speech, Signal Process.*, vol. 1, Apr. 1997, pp. 255–258.
[11] P. Strobach, "Total least squares phased averaging and 3-D ESPRIT for joint azimuth-elevation-carrier estimation," *IEEE Trans. Signal Process.*, vol. 49, no. 1, pp. 54–62, Jan. 2001.
[12] L. Y. Xu, X. F. Zhang, and Z. Z. Xu, "Joint 2D angle and frequency estimation method based on parallel factor quadrilinear decomposition," *J. Electron. Inf. Technol.*, vol. 33, no. 8, pp. 1889–1894, 2011.
[13] L. Y. Xu, X. F. Zhang, and Z. Z. Xu, "Joint 2D angle and frequency estimation based on uniform square array," *J. Appl. Sci.*, vol. 29, no. 2, pp. 187–194, 2011.
[14] J. B. Kruskal, "Three-way arrays: Rank and uniqueness of trilinear decompositions, with application to arithmetic complexity and statistics," *Linear Algebra Appl.*, vol. 18, no. 2, pp. 95–138, 1975.
[15] N. D. Sidiropoulos, L. De Lathauwer, X. Fu, K. Huang, E. E. Papalexakis, and C. Faloutsos, "Tensor decomposition for signal processing and machine learning," *IEEE Trans. Signal Process.*, vol. 65, no. 13, pp. 3551–3582, Jul. 2017.

[16] L. Y. Xu, X. F. Zhang, and Z. Z. Xu, "Novel blind joint 2D direction of arrival and frequency estimation with L-shaped array," *Int. J. Digit. Content Technol. Appl.*, vol. 5, no. 9, pp. 241–250, 2011.
[17] X. Zhang, G. Feng, J. Yu, and D. Xu, "Angle–frequency estimation using trilinear decomposition of the oversampled output," *Wireless Pers. Commun.*, vol. 51, no. 2, pp. 365–373, 2009.
[18] X. Zhang, D. Wang, and D. Xu, "Novel blind joint direction of arrival and frequency estimation for uniform linear array," *Prog. Electromagn. Res.*, vol. 86, pp. 199–215, Jan. 2008.
[19] D. L. Donoho, "Compressed sensing," *IEEE Trans. Inf. Theory*, vol. 52, no. 4, pp. 1289–1306, Apr. 2006.
[20] M. A. Forbes and A. Shpilka, "On identity testing of tensors, low-rank recovery and compressed sensing," in *Proc. 44th Annu. ACM Symp. Theory Comput.*, 2011, pp. 163–172.
[21] S. Li, L. Da Xu, and X. Wang, "Compressed sensing signal and data acquisition in wireless sensor networks and Internet of Things," *IEEE Trans. Ind. Inform.*, vol. 9, no. 4, pp. 2177–2186, Nov. 2013.
[22] N. D. Sidiropoulos and A. Kyrillidis, "Multi-way compressed sensing for sparse low-rank tensors," *IEEE Signal Process. Lett.*, vol. 19, no. 11, pp. 757–760, Nov. 2012.
[23] S. Li, Z. Z. Sun, X. F. Zhang, and D. Z. Xu, "Joint DOA and frequency estimation for linear array with compressed sensing PARAFAC framework," *J. Circuits Syst. Comput.*, vol. 26, no. 9, pp. 1–22, 2017.
[24] P. Stoica and A. Nehorai, "Performance study of conditional and unconditional direction-of-arrival estimation," *IEEE Trans. Acoust., Speech Signal Process.*, vol. 38, no. 10, pp. 1783–1795, Oct. 1990.
[25] P. Stoica and N. Arye, "MUSIC, maximum likelihood, and Cramer-Rao bound," *IEEE Trans. Acoust., Speech Signal Process.*, vol. 37, no. 5, pp. 720–741, May 1989.
[26] P. Stoica and A. Nehorai, "MUSIC, maximum likelihood and Cramer-Rao bound: Further results and comparisons," in *Proc. Int. Conf. Acoust., Speech, Signal Process. (ICASSP)*, vol. 4, May 1989, pp. 2605–2608.
[27] X. Zhang, J. Li, and L. Xu, "Novel two-dimensional DOA estimation with L-shaped array," *EURASIP J. Adv. Signal Process.*, vol. 2011, Dec. 2012, Art. no. 50.
[28] Y. Hua, T. K. Sarkar, and D. D. Weiner, "An L-shaped array for estimating 2-D directions of wave arrival," *IEEE Trans. Antennas Propag.*, vol. 39, no. 2, pp. 143–146, Feb. 1991.
[29] L. Y. Xu, X. F. Zhang, Z. Z. Xu, and M. Yu, "Joint 2D-DOA and frequency estimation for L-shaped array using iterative least squares method," *Int. J. Antennas Propag.*, vol. 2012, Jul. 2012, Art. no. 983092.
[30] S. Li and X. Zhang, "Study on the compressed matrices in compressed sensing trilinear model," *Appl. Mech. Mater.*, vols. 556–562, pp. 3380–3383, May 2014.
[31] T. D. Pham and J. Möcks, "Beyond principal component analysis: A trilinear decomposition model and least squares estimation," *Psychometrika*, vol. 57, no. 2, pp. 203–215, 1992.
[32] N. D. Sidiropoulos and X. Liu, "Identifiability results for blind beamforming in incoherent multipath with small delay spread," *IEEE Trans. Signal Process.*, vol. 49, no. 1, pp. 228–236, Jan. 2001.
[33] L. Huang, T. Long, E. Mao, and H. C. So, "MMSE-based MDL method for robust estimation of number of sources without eigendecomposition," *IEEE Trans. Signal Process.*, vol. 57, no. 10, pp. 4135–4142, Oct. 2009.
[34] T. Huang *et al.*, "Adaptive matching pursuit with constrained total least squares," *EURASIP J. Adv. Signal Process.*, vol. 2012, Apr. 2012, Art. no. 76.

LE XU received the B.E. degree from the Nanjing University of Aeronautics and Astronautics, Nanjing, China, in 2016, where he is currently pursuing the master's degree in communication and information systems with the College of Electronic and Information Engineering. His current research interests include array signal processing and compressed sensing theory.

RIHENG WU (M'12) received the Ph.D. degree in measurement technology and instruments from the Beijing Institute of Technology, Beijing, China, in 2007. He was a Research Associate Fellow with the Department of Electrical Engineering and Computer Science, The University of Tennessee, Knoxville, TN, USA, from 2007 to 2008. From 2009 to 2015, he was with hi-tech companies in Kansas, MO, USA, including Garmin International, Inc., and so on, where he owned two authorized U.S. patents. Since 2016, he has been with the Information Engineering Department, Wenjing College, Yantai University, Yantai, China, where he is currently a Full Professor. His recent research interests include generic signal processing in communication and radar, high-resolution imaging for real-beam radar, array signal processing, and millimeter-wave radar.

Dr. Wu serves as a member of the Technical Program Committees of numerous IEEE conferences, including ICC (2011 and 2012), WCNC (2009, 2010, 2011, 2012, 2013, and 2017), CCNC (2011, 2012, and 2018), APMC2017, and VTC.

He serves as an Editor for the Magazine of the IEEE Vehicular Technology Society (2010), the *International Journal of Computing and Digital Systems-V7* (2018), and the *Journal of Engineering and Computer Innovations*.

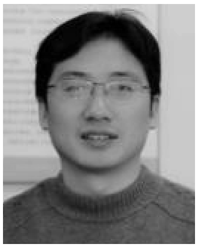

XIAOFEI ZHANG received the M.S. degree from Wuhan University, Wuhan, China, in 2001, and the Ph.D. degree in communication and information systems from the Nanjing University of Aeronautics and Astronautics, Nanjing, China, in 2005. He is currently a Full Professor with the Electronic Engineering Department, Nanjing University of Aeronautics and Astronautics. His research is focused on array signal processing and communication signal processing.

Dr. Zhang serves on the Technical Program Committees of the IEEE 2010 International Conference on Wireless Communications and Signal Processing (WCSP), SSME 2010, the IEEE 2011 WCSP, and the 2011 International Workshop on Computation Theory and Information Technology.

He serves as an Editor for the *International Journal of Digital Content Technology and its Applications*, the *International Journal of Technology and Applied Science*, the *Journal of Communications*, *Information Sciences*, the *Scientific Journal of Microelectronics*, and the *International Journal of Information Engineering*.

He also serves regularly as a Peer Reviewer for the IEEE TRANSACTIONS WIRELESS COMMUNICATION, the IEEE TRANSACTIONS ON VEHICULAR TECHNOLOGY, the *EURASIP Journal on Advances in Signal Processing*, the IEEE COMMUNICATION LETTERS, *Signal Processing*, the *International Journal of Electronics*, the *International Journal of Communication Systems*, and *Wireless Communications and Mobile Computing*.

ZHAN SHI received the B.E. degree from the Nanjing University of Aeronautics and Astronautics, Nanjing, China, in 2016, where he is currently pursuing the Ph.D. degree in communication and information systems with the College of Electronic and Information Engineering. His current research interests include array signal processing.